9

Cyclodextrins, Cyclomannins, and Cyclogalactins with five and six (1→4)-linked Sugar Units : an Assessment of their Conformations and Hydrophobicity Patterns

Abstract: A molecular modeling study of the (1→4)-linked cyclooligosaccharides containing five and six α-D-glucose, α-D-mannose, and β-D-galactose units, respectively, provides a clear conception of their overall conformations, their contact surfaces, and their cavity proportions. A MOLCAD-based generation of their molecular lipophilicity patterns (MLP's) gives a lucid picture of their hydrophobic and hydrophilic surface areas, and hence, a first estimation of their inclusion properties.

The naturally occurring cyclodextrins **2** – **5** are a group of cyclic oligosaccharides containing six, seven, eight or nine α(1→4)-linked D-glucopyranose units per molecule, which have unusual loop structures – a feature that allows them to form inclusion complexes by insertion of a wide variety of organic molecules into their hydrophobic intramolecular cavity[305-308]. These few starch-derived cyclodextrins have been complemented by an imposing number of chemically modified analogs – configurational isomers as well as various deoxy-, amino-, thio-, and epoxy derivatives[308,427] – and in considerably increasing measure recently by chemical synthesis, i.e. via cyclization of linear oligosaccharides. Through the latter approach, various non-natural cyclodextrins (as a generic name for cycloglucooligosaccharides) became available: **1** with five α(1→4)-linked glucose residues[442], the α(1→6)-analogs with three, four, and six glucose units[461], and a β(1→3)-cyclogluco-hexaoside[462].

Cyclodextrins

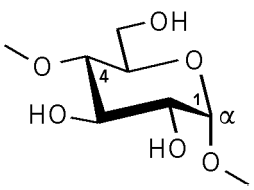

	1	*cyclo*[D-Glc*p*α(1→4)]$_5$
α-CD	**2**	*cyclo*[D-Glc*p*α(1→4)]$_6$
β-CD	**3**	*cyclo*[D-Glc*p*α(1→4)]$_7$
γ-CD	**4**	*cyclo*[D-Glc*p*α(1→4)]$_8$
δ-CD	**5**	*cyclo*[D-Glc*p*α(1→4)]$_9$

Cyclomannins

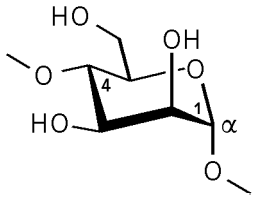

6	*cyclo*[D-Man*p*α(1→4)]$_5$
7	*cyclo*[D-Man*p*α(1→4)]$_6$
8	*cyclo*[D-Man*p*α(1→4)]$_7$
9	*cyclo*[D-Man*p*α(1→4)]$_8$

Cyclogalactins

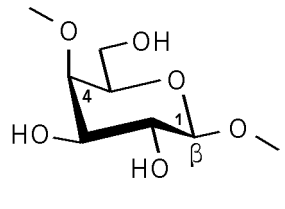

10	*cyclo*[D-Gal*p*β(1→4)]$_5$
11	*cyclo*[D-Gal*p*β(1→4)]$_6$
12	*cyclo*[D-Gal*p*β(1→4)]$_7$

Also, the four cyclomannins **6 – 9** composed of five, six, seven, and eight α(1→4)-linked mannoses have been synthesized[443-446]. In the respective (1→4)-linked cyclogalactins **10 – 12**, as yet unknown, both linkage centers – as compared with their cyclodextrin counterparts **1 – 3** – are inverted: the 4-OH is axially oriented, and the anomeric configuration must necessarily be β, an "*inverso*-cyclodextrin", so to say.

Nomenclature: As cyclodextrins derive their name from dextrose, an early synonym for glucose, those cyclooligosaccharides consisting of mannose, galactose, and allose may accordingly be named as cyclomannins, cyclogalactins, and cycloallins. As this terminology leads to considerable simplifications in the exasperating task of naming these compounds, it is encouraging to propose its use.

The traditional names for the starch-derived cyclodextrins use Greek letters for their differentiation, i.e. α-CD through δ-CD for those containing 6 – 9 glucose units. Whilst this is standard usage, and hence, to be maintained, it appears unreasonable to adhere to the Greek alphabet with other cyclooligosaccharides, not only because this does not reveal ring size or the number of sugar units in a direct way, but it runs into basic difficulties in naming cyclodextrins or analogs smaller than α, as for example, **1**, **6**, and **10**. On the other hand, chemical names such as cyclomaltohexaose for the α-CD (**2**) induce confusion as to the number of maltose units in the ring (six ?), since its all-*manno* analog **7** has quite logically been designated as cyclo-α(1→4)-mannohexaose. In addition, prevailing carbohydrate nomenclature requires for oligosaccharides the ending -oside rather than -ose which indicates a free anomeric center, and this should logically be applied to cyclooligosaccharides as well.

To establish consistency, it is proposed to use the term cyclodextrin as a generic name for all cyclooligosaccharides composed of glucose units, and cycloglucooligosaccharide with the type of intersaccharidic linkage inserted as the specific designation. This entails the term cyclo-α(1→4)-glucohexaoside for α-CD (**2**), and cyclo-α(1→6)-glucotrioside for the rather peculiar cycloisomaltotrioside[461b]. Other exemplary cases are outlined in the following summary:

generic name	specific name	abbreviation *	ref.
cyclodextrin	cyclo-α(1→4)-glucohexaoside (**2**)	*cyclo*[Glc*p*α(1→4)]$_6$	306,308
cyclodextrin	cyclo-α(1→6)-glucohexaoside	*cyclo*[Glc*p*α(1→6)]$_6$	461b
cyclodextrin	cyclo-β(1→3)-glucohexaoside	*cyclo*[Glc*p*β(1→3)]$_6$	462
cyclomannin	cyclo-α(1→4)-mannohexaoside (**7**)	*cyclo*[Man*p*α(1→4)]$_6$	445
cyclogalactin	cyclo-β(1→4)-galactohexaoside (**11**)	*cyclo*[Gal*p*β(1→4)]$_6$	–
cyclolactin	cyclo-α(1→4')-lactotrioside	*cyclo*[Gal*p*β(1'→4) Glc*p*α(1→4')]$_3$	444
cyclofructin	cyclo-β(1→2)-fructohexaoside	*cyclo*[Fru*f*β(1→2)]$_6$	447

* The term "*cyclo*" is considered to be a prefix, and hence, is italicized.

If the necessity arises to differentiate between D- and L-sugars, and / or furanose and pyranose forms, the namings are readily specified in more detail, e.g. cyclo-α(1→4)-glucopyranosyl-hexaoside, or *cyclo*[D-Glc*p* α(1→4)]$_6$ for α-CD (**2**).

The number of theoretically possible cyclooligosaccharides is immense, even when limiting them to those containing five, six, and seven sugar units only: five asymmetric centers in a monosaccharide entail $2^5 = 32$ possible isomers per sugar residue, which, when extended to all stereocenters and to the various positional isomers of the sugar units relative to each other, reaches numbers of astronomical dimensions. The definite impossibility to synthesize all of these versus the quest for gaining more insight and eventually a deeper comprehension of the conformations and complexation properties of novel cyclooligosaccharides, necessitates a rigorous restriction of synthetic efforts to those targets, for which – in all probability – basically new features are to be expected. Since their selection inevitably will have to rely on computational methods rather than intuition, a molecular modeling study of a series of cyclic oligosaccharides such as the standard cyclodextrins, their small ring analogs, the cyclofructins, and the all-*manno* and all-*galacto* isomers was set forth. For the (1→4)-linked cyclomannins and cyclogalactins with five and six sugar units each, this chapter provides a first assessment of their conformational and lipophilic features that in part differ substantially from those of the cyclodextrin counterparts.

Conformational Features

Of the (1→4)-linked cyclooligosaccharides listed above, the cyclodextrins **1** and **2**, the cyclomannins **6** and **7**, as well as the cyclogalactins **10** and **11**, each containing either five or six monosaccharide units, were selected for study and subjected to a molecular mechanics analysis with the PIMM91 force field program[45]. Thereby, the molecular parameters

- ω, describing the orientation of the 6-OH group towards the pyranoid ring[66], and
- τ, denoting the tilt of the monosaccharide pyranoid rings towards the macrocycle (cf. Fig. 6-1)

were systematically permuted and finally led to the geometry parameters collected in Table 9-1, and to the global minimum energy conformations in Fig. 9-1, onto which the contact surfaces were superimposed. As a consequence of the structure generation procedure, the PIMM91 minimum energy geometries exhibit symmetrical, almost perfect planar *n*-polygons of the O-1^n-atoms, and hence, can be regarded as time-averaged "molecular images" of solution conformations, respectively[463,].

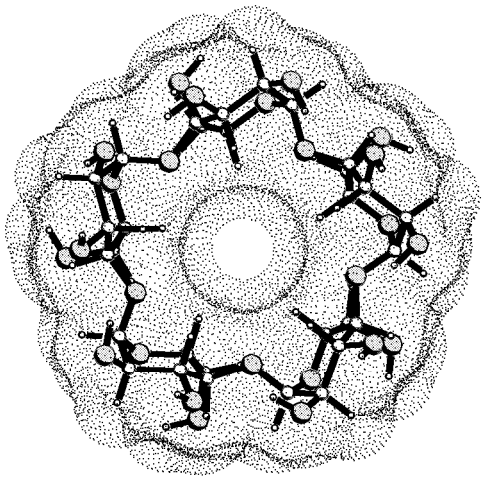

1 *cyclo*[D-Glc*p*α(1→4)]$_5$

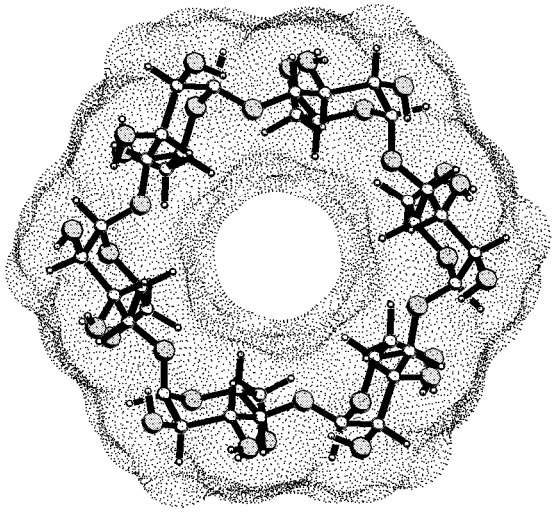

2 *cyclo*[D-Glc*p*α(1→4)]$_6$

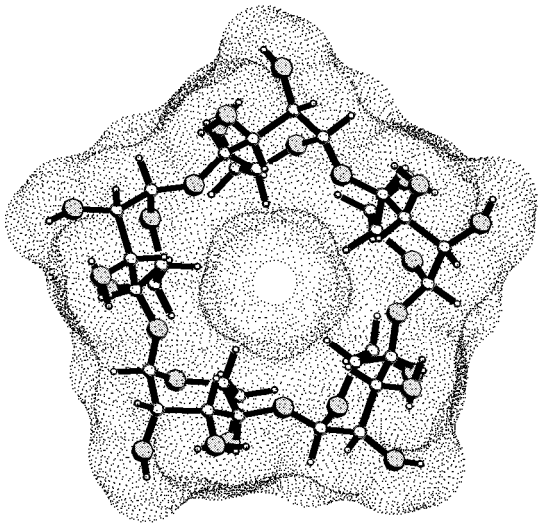

6 *cyclo*[D-Man*p*α(1→4)]$_5$

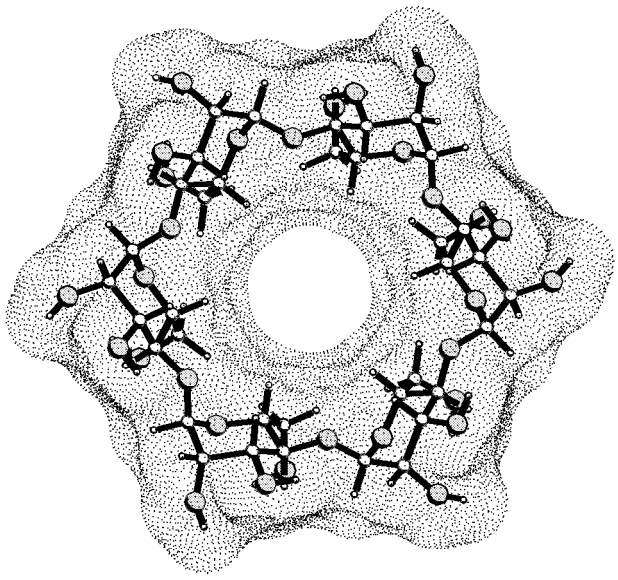

7 *cyclo*[D-Man*p*α(1→4)]$_6$

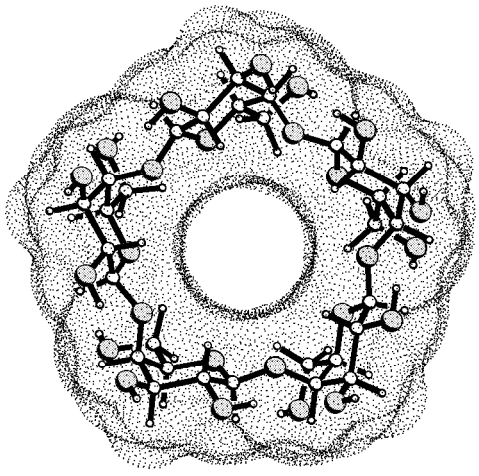

10 *cyclo*[D-Gal*p*β(1→4)]$_5$

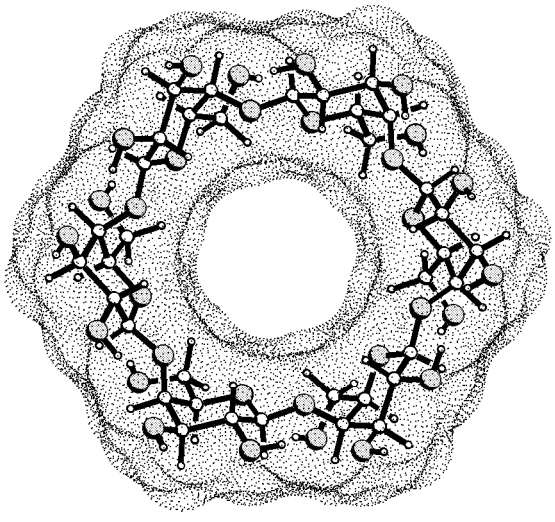

11 *cyclo*[D-Gal*p*β(1→4)]$_6$

Fig. 9-1. (opposite page) Minimum energy structures (PIMM91) and contact surfaces in dotted form for the cyclodextrins (*upper* plots), cyclomannins (*center*), and cyclogalactins (*lower row*) containing five (*left*) and six-monosaccharide units (*right column*), respectively. Structures are shown perpendicular to the mean ring plane of the macrocycles and viewed through the large opening of the conically shaped molecules, i.e. the 2-OH / 3-OH side of the pyranoid rings points towards the viewer, and the primary 6-CH_2OH groups away from him, towards the back.

In each of the cyclooligosaccharides the respective monosaccharide units are positioned in the macrocyclic rings with different tilts and orientations, each of these pyranoid sugars involved is again depicted in enlarged form (Fig. 9-2), in exactly the line of sight as is realized in Fig. 9-1. Thereby, identification of the individual sugar residues in Fig. 9-1 should be greatly facilitated.

The conformation of the pyranoid rings in the three cycloglycohexaosides **2** (α-CD), **7**, and **11** is invariably an essentially unperturbed $^4C_1$ chair, as evidenced by their Cremer-Pople (CP) ring puckering parameters[122,124] listed in Table 9-1 ($\theta \approx 9°$). This also holds true for the respective pentameric analogs **1**, **6**, and **10**, yet the CP angles θ and φ indicate only slight distortions towards the E_1 (in **1**), $^2H_1$ (**6**), and ^4E (**10**) geometries.*

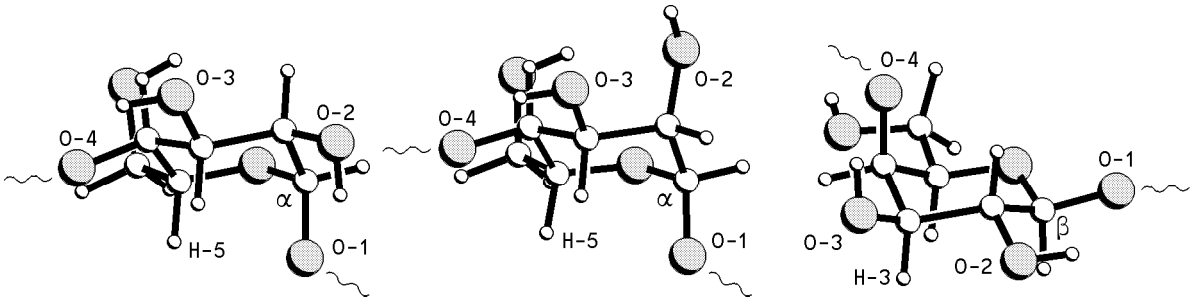

cyclodextrin cyclomannin cyclogalactin

Fig. 9-2. Zoom of the mean monosaccharide units for the minimum energy structures in Fig. 9-1 as seen perpendicular to the cyclooligosaccharide mean plane. Due to the inclination of the pyranoid rings in regard to the macro ring, the α-D-glucosyl and α-D-mannosyl units are seen from their "bottom" sides (compare to the residue geometries in top right corner of the cyclohexaoside structures in Fig. 9-1), whereas the β-D-galactosyl residue (bottom left unit of *cyclo*[Galβ(1→4)]$_6$ in Fig. 9-1) corresponds to the conventional depiction of a $^4C_1$ pyranose conformation.

---

* Most notably, distortions of the pyranose units (increasing θ) occur at opposite ring carbons involved in the equatorial part the intersaccharidic linkage, i.e. C-4 in cycloglucosides and -mannosides ($\phi \approx 70 - 100°$), and C-1 of the cyclogalactosides ($\phi \approx 230°$), respectively. Flattening of this center is energetically more favorable than bending of the axial position, since the adjacent pyranose ring torsion angles decrease rather than increase.

In the case of the two cyclodextrins, on going from the hexameric α-CD (**2**) to the cycloglucopentaoside **1**, the average tilt – i.e. the inclination of the pyranoid rings towards the mean plane of the macrocycle – decreases by about 7° (from 109.0° to 101.7°, cf. Table 9-1), signifying that the upper rim 2-OH / 3-OH groups are shifted more to the inside on expense of a widening at the lower rim-aperture where the 6-CH_2OH residues as situated. This is obviously caused by the necessity to release the steric congestion produced by the inside-pointing 5-hydrogens in **1** as compared to α-CD (**2**). This also has consequences for the intersaccharidic torsion angles: Φ in widened from ≈ 95° for α-CD (**2**) to ≈ 102° for the pentamer **1**, correspondingly Ψ becomes smaller (≈ 138° → ≈ 133°). Also, the mean distances between O-2 and O-3 of adjacent glucose units are slightly shortened in **1** as compared to α-CD (**2**), and simultaneously, the C-6 – C-6'-distances at the opposite torus-rim increase (≈ 4.2 Å for **2** versus ≈ 4.5 Å in **1**).

When comparing the two cyclomannins **6** and **7** to the cyclodextrin analogs **1** and **2**, they have very similar backbone structures, indicating that inversion of the 2-OH group in the pyranoid rings exerts no major effect thereupon. The mean tilt angles τ for **6** and **7** turn out to be very similar and find expression in – compared to **1** and **2** – inverse changes in Φ and Ψ, which now reflect the geometrical constraints of the cyclopentaoside **6** in relation to the hexamer **7**.

Basically different are the conformations of the two cyclogalactins **10** and **11**. Due to the epimerization at C-4 and the anomeric center these "*inverso*-cyclodextrins" have an inverse orientation of the pyranoid rings in the macrocycle. Unlike the cyclodextrins, where H-2, H-4, and the pyranoid ring oxygen point towards the outside, in the cyclogalactins H-2 and the ring oxygen are directed towards the inside, towards the center cavity. This makes the cavities in **10** and **11** less congested by axial hydrogen atoms than in the case of the cyclodextrins and cyclomannins (there H-3 and H-5 are inside the cavity). Accordingly, the cavities of the two cyclogalactins are not only wider than those of their glucose and mannose analogs, but they are distinctively more uniform, adopting a rod-shape appearance (cf. Fig. 9-3).

With respect to intramolecular hydrogen bonding of the OH ··· O-type, it is well established that these prevail between the adjacent 2-OH / 3-OH groups in cyclodextrins in the solid state[327,328] as well as in solution[329]. A consequence thereof is the chemical inertness of the 3-OH groups[329], as well as the remarkably high 2-*O*-selectivity of base-induced alkylations – the alkoxide anion is most efficiently stabilized by an intramolecular H-bond at the O-2-position[330]. In the cyclomannins, inversion at C-2 results in O_2-$O_{3'}$-distances (cf. Table 9-1) too large to

be compatible with interresidue hydrogen bonding, while for the cyclogalactins similar effects as in the cyclodextrins are to be expected.

Table 9-1. Mean molecular geometry parameters of the PIMM91-calculated conformations for the cyclooligosaccharides with five and six (1→4)-linked glucose (**1**, α-CD **2**), mannose (**6**, **7**), and galactose units (**10**, **11**).

compound	torsion angles[a]		angle[b]	tilt[c]	distances [Å]		
	<Φ>	<Ψ>	<φ>	<τ>	$<O_1\text{-}O_{1n'}>$[d]	$<O_2\text{-}O_{3'}>$	$<C_6\text{-}C_{6'}>$
1	102.4(0.7)	133.2(1.1)	117.8(0.2)	101.7(0.6)	6.53(0.02)	3.21(0.06)	4.51(0.01)
2 α-CD	95.4(0.3)	138.7(1.1)	117.3(0.2)	109.0(0.2)	8.74(0.03)	3.30(0.04)	4.19(0.01)
6	83.2(0.1)	152.2(0.1)	119.3(0.1)	112.7(0.1)	7.09(0.01)	5.65(0.01)	4.16(0.01)
7	88.6(0.1)	145.5(0.1)	117.4(0.1)	113.8(0.1)	9.01(0.01)	5.45(0.01)	4.12(0.01)
10	-89.6(1.5)	-150.7(1.8)	121.5(0.4)	-104.8(1.0)	6.91(0.05)	3.42(0.10)	4.60(0.02)
11	-92.2(1.5)	-147.0(1.5)	118.8(0.3)	-108.7(1.1)	8.92(0.03)	3.39(0.09)	4.45(0.02)

compound	torsion angles[a]		Cremer-Pople parameters			monosaccharide conformation
	$<\Theta_1>$	$<\Theta_2>$	<Q>	<θ>	<ϕ>	
1	39.4(0.9)	-39.6(0.1)	0.544(0.004)	18.0(0.2)	67.1(4.8)	$^4C_1$ ($\rightarrow$ E_1)
2 α-CD	46.9(0.7)	-47.0(0.2)	0.550(0.002)	9.0(0.3)	74.3(6.1)	$^4C_1$
6	45.4(0.1)	-40.1(0.1)	0.544(0.001)	15.4(0.1)	97.2(0.1)	$^4C_1$ ($\rightarrow$ $^2H_1$)
7	49.3(0.1)	-46.0(0.1)	0.552(0.001)	9.7(0.1)	104.8(0.1)	$^4C_1$
10	59.7(0.8)	-61.1(0.3)	0.562(0.006)	13.1(0.1)	232.0(5.2)	$^4C_1$ ($\rightarrow$ ^4E)
11	57.9(0.4)	-58.4(0.3)	0.559(0.003)	9.1(0.4)	224.0(1.9)	$^4C_1$

Root mean square deviations in parenthesis. – a) Φ: $O_5\text{-}C_1\text{-}O_1\text{-}C_{4'}$, Ψ: $C_1\text{-}O_1\text{-}C_{4'}\text{-}C_{3'}$, Θ_1: $C_2\text{-}C_3\text{-}C_4\text{-}C_5$, Θ_2: $C_3\text{-}C_4\text{-}C_5\text{-}O_5$. – b) φ: $C_1\text{-}O_1\text{-}C_{4'}$. – c) angle between best-fit mean plane of the macro ring (defined by all O_{1n}-atoms) and each monosaccharide-mean plane (atoms $C_1 - C_5$ and O_5). – d) $O_1\text{-}O_{1n'}$-distances (in Å) diagonal across the CD ring.

The conformational preferences of the hydroxymethyl groups in relation to the pyranoid ring[53,67-73] are nearly the same in the cyclodextrin and cyclomannin series: only the *gg* and *gt* conformers are populated, due to 1,3-diaxial-repulsions between O-4 and O-6 in the alternative *tg* rotamer. In the case of the *gg* arrangement the respective OH groups are directed towards the outside of the macrocycles, whilst the *gt* rotamers point the 6-OH groups towards the center. In the cyclogalactins, the *tg* and *gt* rotamers are favored and are both directed away from the molecular center. In the PIMM91 calculations the *tg* form emerges as the most stable conformer.

Contact Surfaces and Cavity Proportions

Molecular contact surfaces[46], which are closely related to the solvent-accessible surfaces[47], better display steric features than atomic distance parameters can do. Based on the conformations calculated for the six cyclooligosaccharides, their respective contact surfaces were generated by the MOLCAD-program[48] and depicted in dotted form (Fig. 9-1). For better visualization of the extension of these surfaces and the cavity proportions, cross cuts through the contact surfaces are given in Fig. 9-3, the respective contour lines originate from successive 10° rotation steps around the geometrical center *M* (cf. Fig. 6-7). The approximate spatial distances are inserted in Fig. 9-3, surface dimensions and volumes of the cyclodextrins and the cavities are contained in Table 9-2 (for definition of the cavity see Fig. 8-6).

As is clearly apparent from Fig. 9-3, the two cyclodextrins and cyclomannins resemble each other closely with respect to their overall shape and, most notably, the form of their cavities. The respective pentamers **1** and **6** (left entries in Fig. 9-3) – obviously as a result of the respective H-5 atoms extending more closely into the cavity than in their hexameric analogs **2** (α-CD) and **7** (right) – show a pronounced protrusion of the surface towards the center of the cavity. This indentation is expected to have major bearing on their ability to form inclusion complexes, inasmuch as the binding of hosts requires penetration into the cavity (e.g. sodium 1-propanesulfonate in α-CD[407]) and thus, will be highly unlikely, and threading of **1** and **6** on polymer chains – possible with α-CD (**2**)[308] – should essentially be impossible. These limitations do not apply to the cyclogalactins **10** and **11**, since both feature more channel-shaped cavities, wider in each case than those of their gluco- or manno-counterparts.

Table 9-2. Molecular dimensions, surface areas, and volumes of cyclodextrins **1** and **2**, cyclomannins **6** and **7**, and cyclogalactins **10** and **11**.

compound		torus ∅ [Å]		torus	surface area [Å²]		molecular volume [Å³]	
		outer	inner	height	total	cavity	total	cavity
1		12.6	3.9	8.0	605	60	815	50
2	α-CD	14.2	5.2	8.0	720	85	975[464]	100
6		13.1	3.8	7.4	620	65	810	50
7		14.9	5.1	7.4	730	85	970	100
10		12.6	3.8	8.0	625	60	815	60
11		14.1	5.4	8.0	735	90	970	120

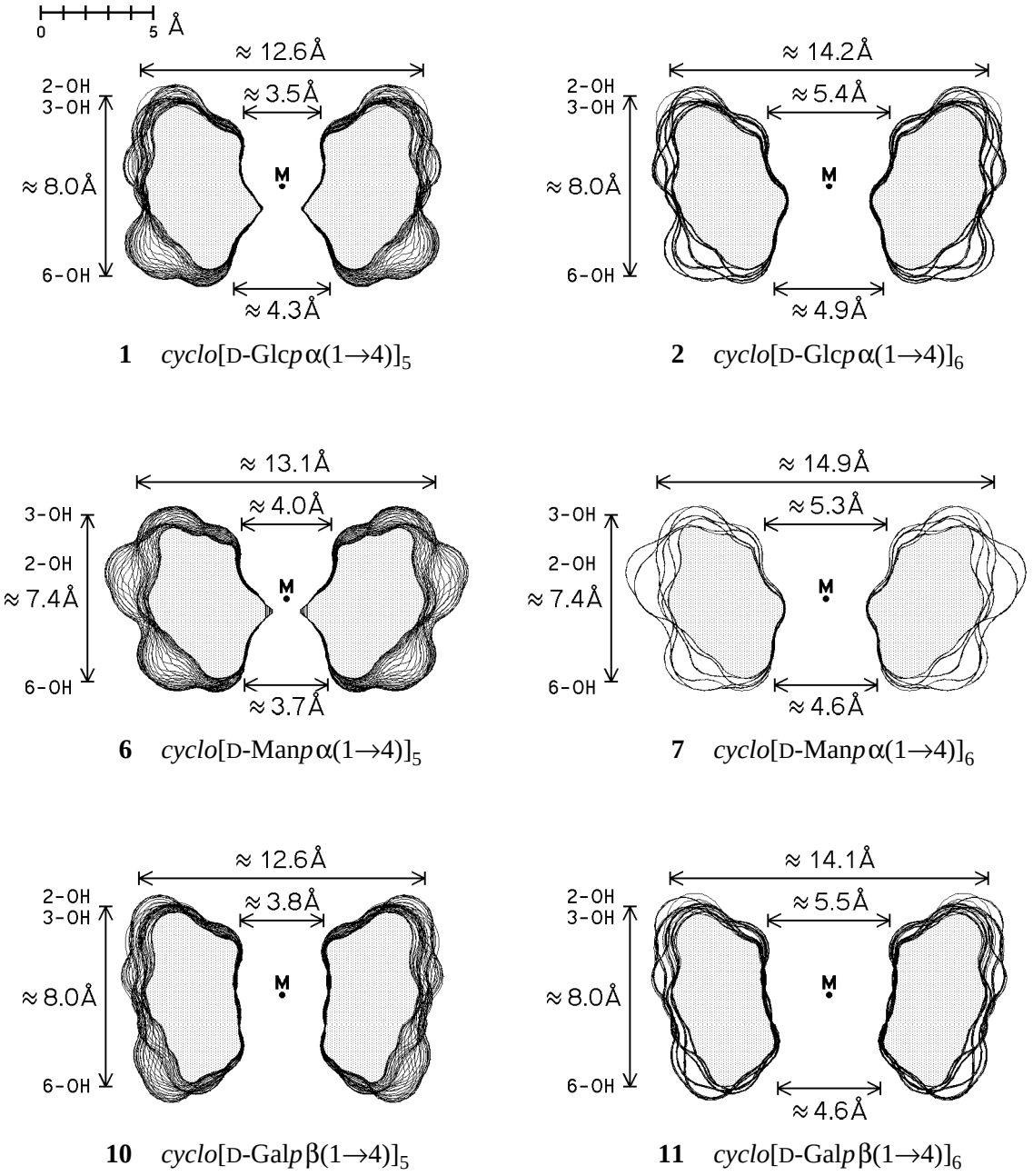

1 *cyclo*[D-Glc*p*α(1→4)]$_5$ **2** *cyclo*[D-Glc*p*α(1→4)]$_6$

6 *cyclo*[D-Man*p*α(1→4)]$_5$ **7** *cyclo*[D-Man*p*α(1→4)]$_6$

10 *cyclo*[D-Gal*p*β(1→4)]$_5$ **11** *cyclo*[D-Gal*p*β(1→4)]$_6$

Fig. 9-3. Cross cut plots (cf. Fig. 6-7) through the contact surfaces and approximate molecular dimensions of the (1→4)-linked cyclodextrins (**1** and **2**, *top*), cyclomannins (**6** and **7**, *middle*), and cyclogalactins (**10** and **11**, *bottom*). The contour lines result from successive 10° rotation steps around the geometrical center *M*. In each case, the larger opening (top side) of the conically shaped molecules carries the secondary 2-OH and 3-OH at the torus rim, whilst the primary 6-OH groups are positioned at the opposite (bottom) side forming the rim of the smaller opening.

Another geometrical peculiarity is to be found in the torus heights of these cyclooligosaccharides: it is distinctly smaller in the cyclomannins (7.4 Å for **6** and **7**, versus 8.0 Å each in the cyclodextrins and cyclogalactins, cf. Fig. 9-3) – a finding that also reflected in the smaller cavity surface areas and, more pronouncedly, in the volumes of the cavities. From the calculatory data listed in Table 9-2 it is apparent that the cyclogalactins have an about 20% larger cavity volume than their cyclodextrin and cyclomannin analogs, hence will be anticipated to include correspondingly larger hosts.

Molecular Lipophilicity Profiles

Aside from the imperative fulfillment of steric requirements, the hydrophobic effect[116,117] represents the most important factor in governing guest-host interactions in the cyclodextrin series[305-308]. Concomitantly, the release of complexed water out of the CD cave as well as water from the hydrophobic hydration sphere[117] into the bulk phase must be considered as the main entropic factor favoring complex formation. The color-coded visualization of **m**olecular **l**ipophilicity **p**atterns (**MLP**'s)[58] projected onto the molecular contact surface by using the MOLCAD-molecular modeling program[48,59] is especially suited for the assessment of hydrophobic interactions. The MLP's for the six cyclooligosaccharides are depicted in Figs. 9-4 – 9-7 in a two color code graded into 32 shades, ranging from dark-blue for the most hydrophilic areas to yellow-brown for the most hydrophilic regions (cf. legend to Fig. 9-4). The MLP's of the two cyclodextrins (Fig. 9-4) reveal the 2-OH / 3-OH side of the macrocycles, i.e. the respective wider torus rim, to be distinctly hydrophilic (blue), whereas the narrower opening at the opposite side, made up of five and six 6-CH_2OH groups, is intensely hydrophobic (yellow-brown), extending well into the cavity.

Fig. 9-4. (opposite page). MOLCAD-program generated molecular hydrophobicity (lipophilicity) patterns (MLP's) projected onto the contact surfaces of *cyclo*[Glcα(1→4)]$_5$ (**1**, *left*) and *cyclo*[Glcα(1→4)]$_6$ (**2**, α-cyclodextrin, *right*). Color-coding was carried out cf. footnote on p. 75, blue shading represents most hydrophilic surface areas and yellow-brown colors indicate most hydrophobic regions. The *top* picture views through the larger openings of the conically shaped molecules, exposing the intensively hydrophilic (blue) 2-OH / 3-OH side. In the *middle*, the hydrophilic front half of the surface has been removed providing an inside-view onto the hydrophobic (yellow-brown) backside. In addition, a ball and stick model was inserted to illustrate the molecular orientation (mode of viewing analog to Fig. 9-1). The *bottom* representation depicts the "backside" of the two cyclodextrins (i.e. the smaller opening with the 6-CH_2OH groups facing the viewer), clearly exposing the hydrophobic (yellow-brown) surface areas that extend well into the cavity.

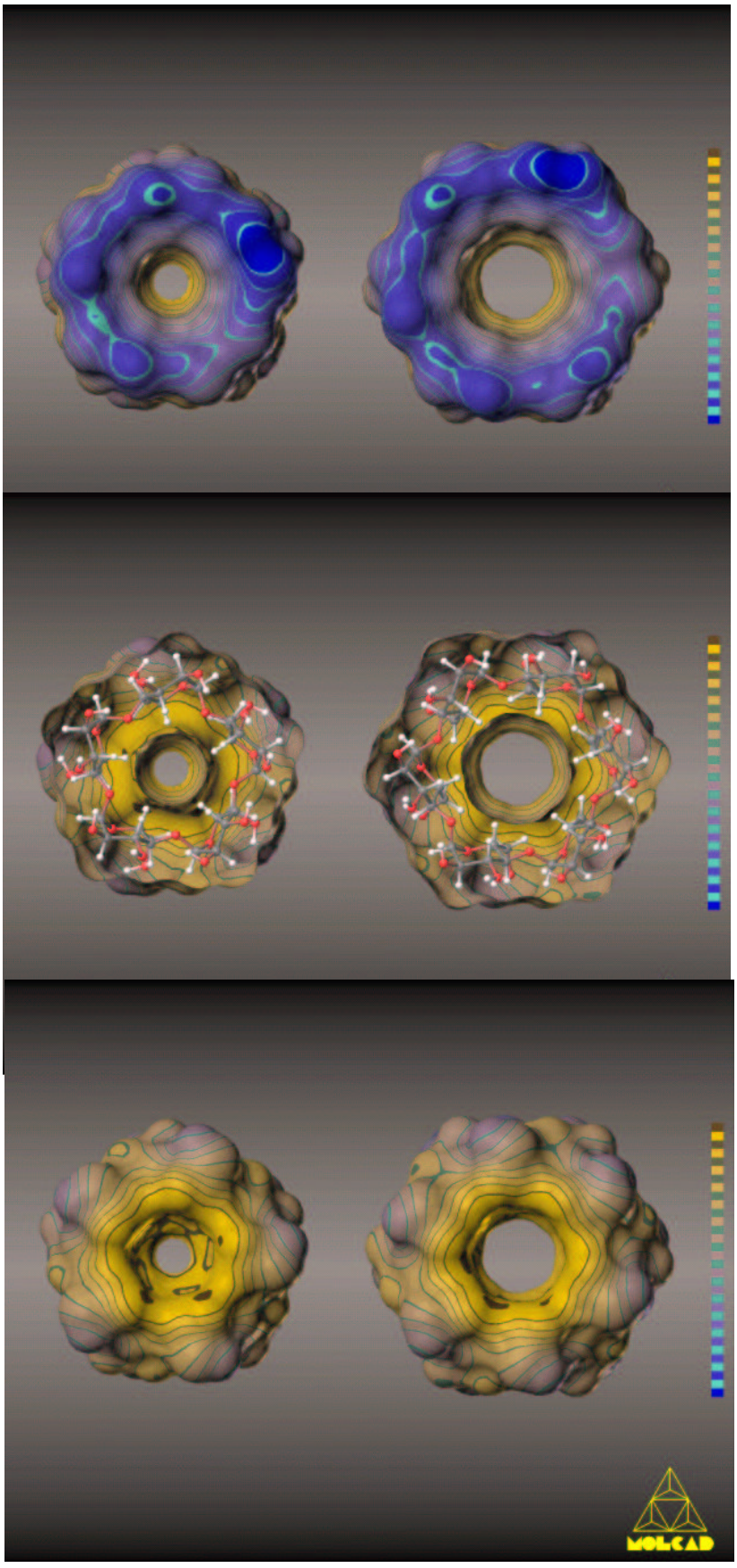
MOLCAD

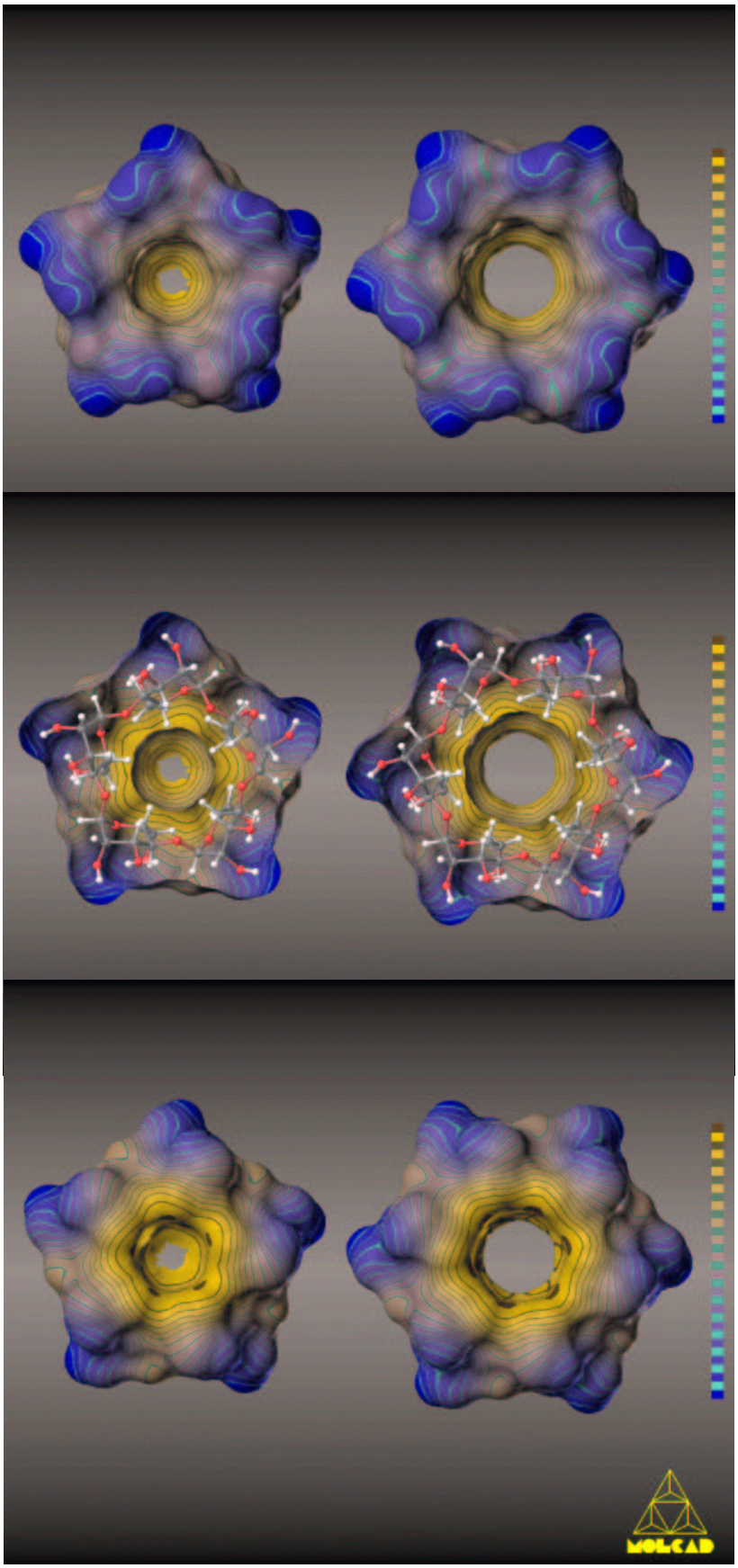

Fig. 9-5. MLP's of the cyclomannins with five (**6**, *left*) and six (**7**, *right*) α(1→4)-linked mannose units, respectively; molecular orientation and mode of visualization as in Fig. 9-1 and 9-4.

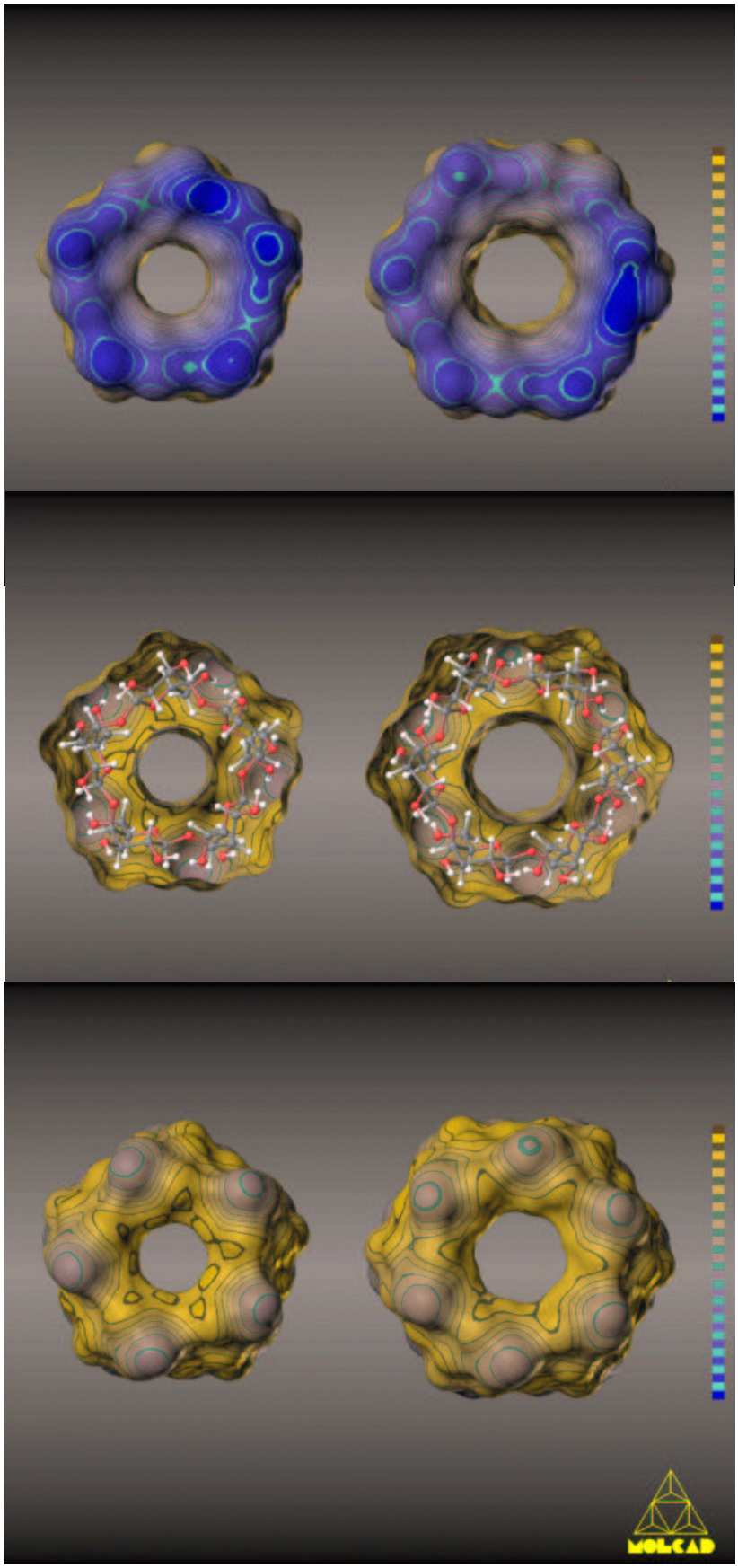

Fig. 9-6. MLP's of the β(1→4)-cyclogalactins **10** and **11**, composed of five (*left*) and six (*right*) galactose residues. Mode of viewing as in Fig. 9-1 and 9-4.

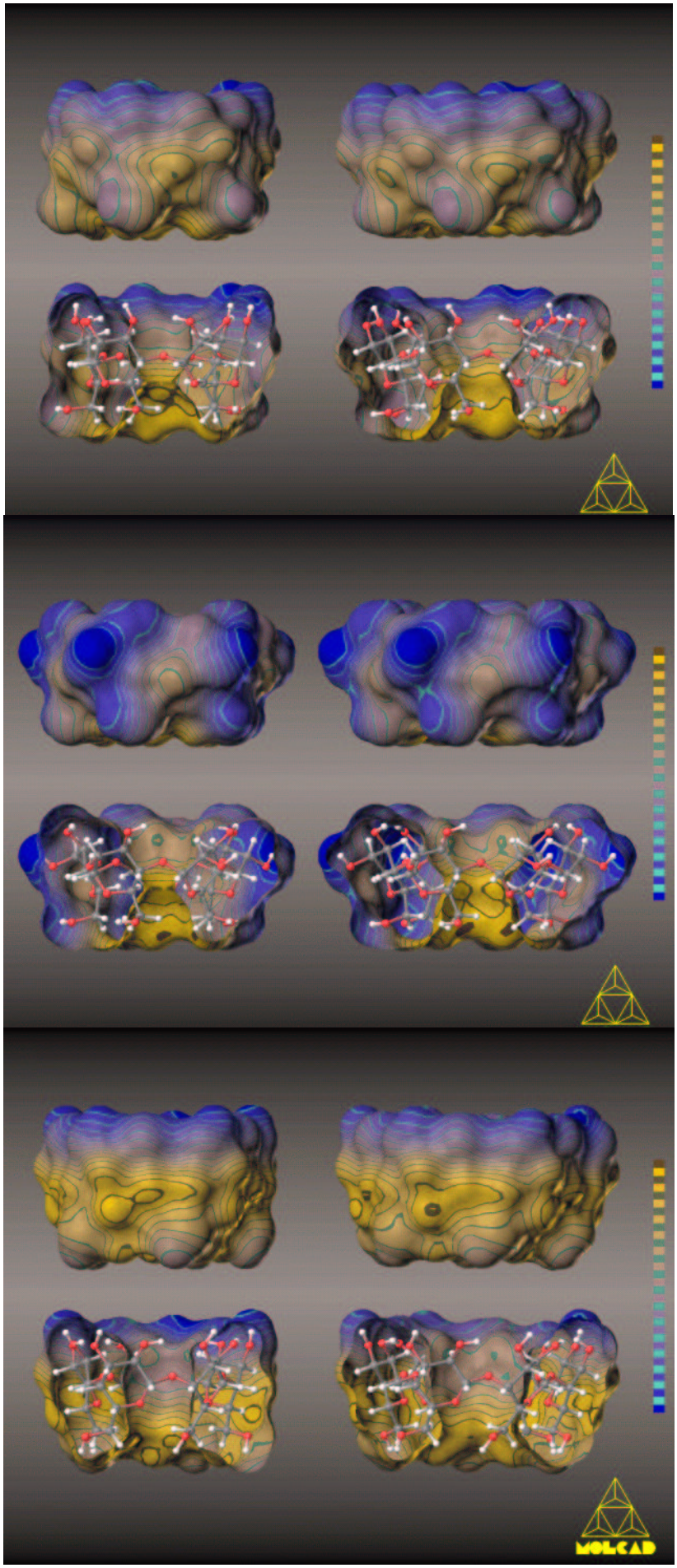
MOLCAD

Fig. 9-7. (opposite page). Side view MLP's (color-coding cf. Fig. 9-4), in closed and bisected form each, of the two α(1→4)-cyclodextrins **1** and **2** with five (*left*) and six (*right*) glucose units (*top* picture), and their respective α(1→4)-cyclomannin (**6** and **7**, *middle*) and β(1→4)-cyclogalactin analogs (**10** and **11**, *bottom*). Their orientation is uniformly such, that the 2-OH / 3-OH side is aligned upward (larger opening of the torus) and the 6-CH_2OH points downward (smaller aperture). The differences in their hydrophilic (blue) and hydrophobic surface areas – most notably on the inside regions of their cavities – are clearly apparent.

An even more articulate impression of the MLP's of the cyclodextrins is provided by the juxtaposition of the respective side-views in closed and half-opened form (Fig. 9-7, top entry).

The two cyclomannins **6** and **7** show a quite similar distribution of hydrophilic and hydrophobic regions, yet inspection of the side-view (Fig. 9-7, middle section) reveals the entire outside to be essentially more hydrophilic (in relative terms) than the respective outer surfaces of the cyclodextrins. Accordingly, the cavity areas in the cyclomannins are conceivably more hydrophobic than that of the cyclodextrins. Thus, the capability of the cyclomannins to form inclusion complexes is characterized by – as compared to the respective cyclodextrins – a smaller, yet more hydrophobic cavity.

In the cyclogalactins **10** and **11** the situation is – not unexpectedly – distinctly different (Fig. 9-6). As *inverso*-cyclodextrins, the "cyclic ribbon" of the five resp. six interlinked pyranoid chairs is turned inside-out, entailing the 6-CH_2OH-side (Fig. 9-6, lower entry) to have substantially enlarged hydrophobic surface areas that extend from the cavity well beyond the rim to the outside of the macrocycles. This becomes even more apparent from the side views of **10** and **11** given in Fig. 9-7 (bottom section). Accordingly, these cavities are less hydrophobic – in relative terms – than those of their glucose and mannose counterparts. Thus, the efficiency with which these two cyclogalactins are apt to form inclusion complexes is determined by two factors: wider, but less hydrophobic cavities than those in the corresponding cyclodextrins and cyclomannins – hence their potential for including larger hosts that may even be slightly hydrophilic.

These rationalizations are by intention kept very general and are not carried into details. For further interpretations and, particularly, for speculations there is ample room, which at the present state of the knowledge is deliberately refrained from using.

Appendix – Computational Methods

The following computational methods were used:

I. Monosaccharide Tilt Angle τ Variations. Standard PIMM91-optimized $^4C_1$-conformations of α-D-glucose, α-D-mannose, and β-D-galactose with different hydroxymethyl torsions ω (cyclodextrins and cyclomannins: *gg*, ω = -60°, and *gt*, ω = +60°; cyclogalactins: *tg*, ω = ±180°, and *gt*, ω = +60°)[66] were pieced together by a rigid body rotation and fitting procedure[128] to form a regular *n*-polygon with the O_1 / $O_{4'}$-atoms. Thereby the monosaccharide residue tilt angles τ were varied within the range of +60 – +140° (cyclodextrins and cyclomannins) and -60 – -140° (cyclogalactins) with a stepsize of 5°. After addition of the hydrogen atoms all structures were fully geometry optimized using the PIMM91 force field program[45] (ε = 1), the global minimum energy structures were entered into the molecular modelings.

II. Contact Surfaces and Molecular Lipophilicity Profiles. Calculation of the molecular contact surfaces and the respective hydrophobicity patterns was performed using the MOLCAD[48] molecular modeling program and its texture mapping option[59], a detailed description of the underlying computational basics is given in Chapter 3. Scaling of the MLP's in relative terms was performed for each molecule separately, no absolute values are displayed (overall scaling does not change the graphics significantly). Color graphics were photographed from the computer screen of a SILICON-GRAPHICS workstation.